

A surface energy-budget model coupled with a Skewed Puff Model for investigating the dispersion of radionuclides in a sub-tropical area of Brazil

A. P. OLIVEIRA⁽¹⁾, J. SOARES⁽¹⁾, T. TIRABASSI⁽²⁾ and U. RIZZA⁽³⁾

⁽¹⁾ *Micrometeorology Group, Department of Atmospheric Science, IAG/USP*

Rua do Matão, 1226, CEP 05508.900, São Paulo, SP Brazil

⁽²⁾ *Istituto FISBAT del CNR - Via Gobetti 101, Bologna, Italy*

⁽³⁾ *Istituto ISIAAt del CNR - Via Arnesano, Lecce, Italy*

(ricevuto il 24 Novembre 1997; revisionato l'1 Dicembre 1998; approvato il 22 Dicembre 1998)

Summary. — An air pollution model (Skewed Puff Model, SPM) based on the Monin-Obukhov similarity theory was applied to investigate the atmospheric radionuclide dispersion at Iperó in Brazil, the location of a nuclear industrial installation. The SPM numerical simulations were carried out using as input 5-minute averaged wind speed and direction observed at 11.5 m, friction velocity and the Monin-Obukhov length supplied by the surface energy-budget model, along with PBL height, estimated from empirical equilibrium expressions for the nighttime and Mixed-Layer model for the daytime. The agreement between the observed and simulated sensible and latent heat fluxes, friction velocity and Monin-Obukhov length, within a level of confidence of 99.9% indicates that the internal parameters chosen for the surface energy-budget model are representative of the interface soil-vegetation conditions at Iperó. The mean concentration field at the surface was estimated assuming that a hypothetical accident at Iperó produced a continuous emission from a 10 m high point source for 18 hours during the summer of 1993 and for 36 hours during the winter of 1992. The results indicated that, in the case of an accident, the highest concentration values are located near to the source and most of the contaminated area is within a 5 kilometers range, in both seasons. The shape of the contaminated area is defined by the wind speed pattern.

PACS 92.60 – Air quality and air pollution.

PACS 47.27 – Turbulent flows, convection, and heat transfer.

1. – Introduction

The review on operative atmospheric-dispersion models, provided by Weil [1] in the American Meteorological Society and United States Environmental Protection Agency Workshop, indicates that the Monin-Obukhov similarity theory approach should replace the Pasquill-Gifford stability classification when estimating the turbulence effects on the diffusion of pollutants in the atmosphere. As a consequence, various

organizations worldwide are now introducing advanced modeling techniques which contain algorithms for calculating the main factors determining air pollution diffusion using Monin-Obukhov length scale [2-4].

However, the Monin-Obukhov approach requires information, such as the PBL height and turbulent fluxes at the surface, which are not routinely available. To overcome this difficulty, experimental work and modeling efforts have been performed to parameterize the surface turbulent fluxes in terms of routinely measured elementary meteorological parameters [5-9].

The success of the representation of surface-atmosphere processes is strongly dependent on local conditions. Thus, the appropriate use of the dispersion models in a particular area requires a previous calibration procedure of the algorithm used to estimate the input parameters, which can only be accomplished by field campaigns involving surface layer turbulence measurements and PBL height estimations.

This work reports the calibration of a surface-energy budget model [10] which was employed to estimate surface turbulent fluxes based on a set of detailed turbulence measurements gathered in Brazil. The model output was employed to estimate the height of the PBL, using equilibrium expressions [11] during the nighttime and a Mixed Layer Jump model [12] in the daytime.

The resulting calibrated algorithm (surface energy-budget model and PBL height expressions) was then coupled with a diffusion model (Skewed Puff Model, SPM), in order to investigate the possible patterns and intensity of local environmental contamination by radionuclides. The SPM employs the Monin-Obukhov similarity theory to estimate dispersion conditions and is based on approximated solutions of the air pollution dispersion equation for non-stationary conditions, where particular importance is given to describing the interaction between wind shear and vertical diffusion.

In the present case, the SPM was used to calculate the time-integrated concentration of radionuclides at the surface level, in order to assess the degree of contamination associated to a hypothetical accident in the area of interest, produced by a continuous emission from a 10 m high point source. At this stage of the study, analysis is limited to evaluating the ground level radionuclide concentration and, therefore, no radioactive decay is included.

2. – Observations

The measurements reported here were performed at the Brazilian Navy's industrial installation *Centro Experimental ARAMAR* (CEA). The CEA is located at Iperó in a country region of the State of São Paulo, Brazil (23°25'S and 47°35'W), approximately 120 km from the Atlantic Ocean coastline and 550 m above mean sea level (fig. 1a). The site is located in the central area of the Tietê River valley, which is crossed by the Sorocaba River in the NW-SE direction. The main topographic feature are the 300 m high Araçoiaba Hills in the South-West (fig. 1b).

The area has been the subject of two field campaigns. In both, surface layer turbulence data was obtained from three sets of fast-response sensors at 3.0, 5.0 and 9.4 m above the surface. The sensors measured fluctuations of vertical wind velocity, air temperature and water vapor density with a sampling frequency that varied from 1 to 10 Hz. Net, solar and terrestrial radiation and soil heat flux, temperature and humidity measurements were also carried out [13,14]. Vertical profiles of air temperature,

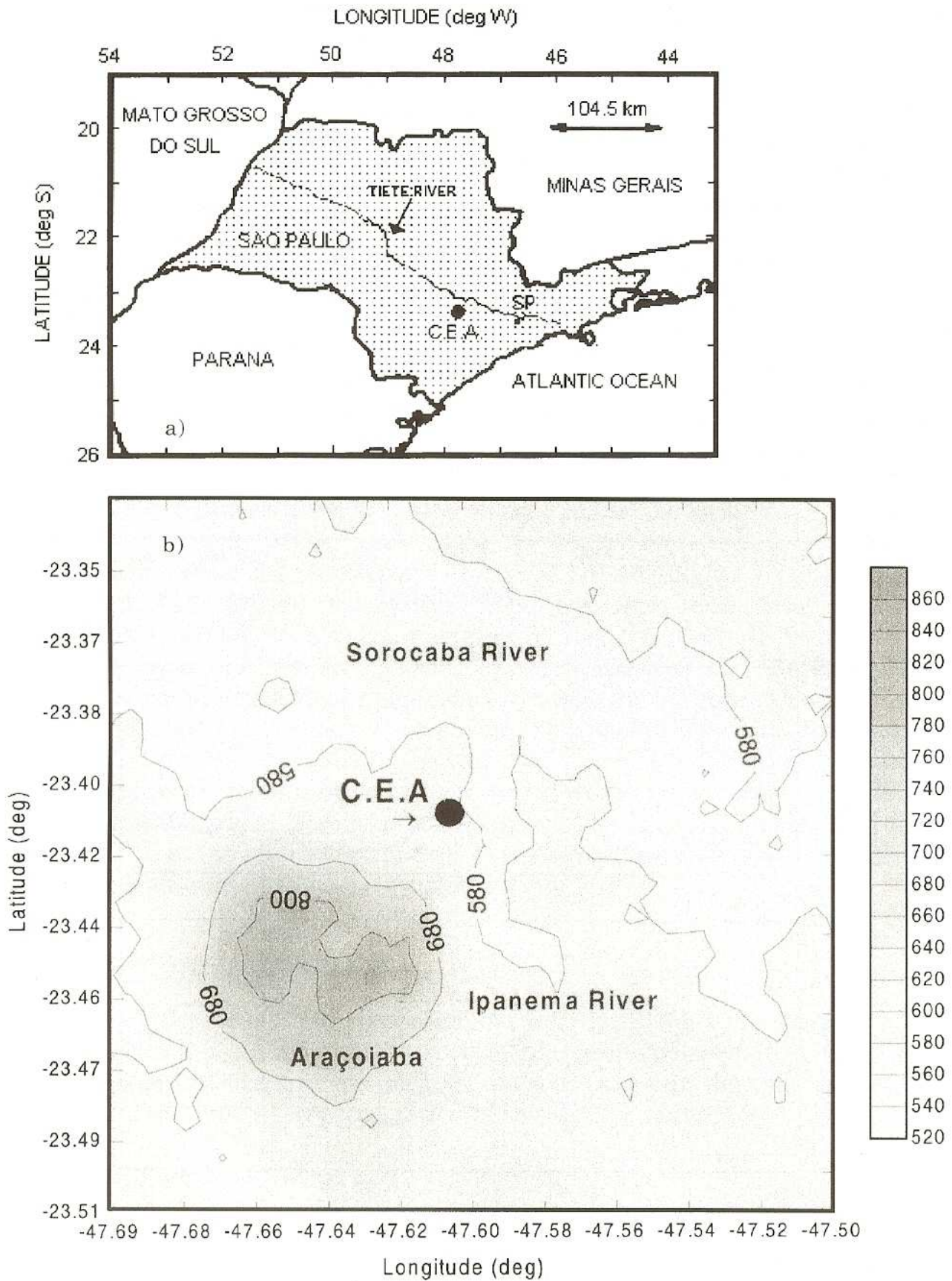


Fig 1. – a) Map of the State of São Paulo. The site is labeled as CEA. The major geographic features are the Tietê River, city of São Paulo labeled as SP and the Atlantic Ocean in the SE portion of the map. b) Topography of the CEA area. The major geographic features are the Sorocaba and Ipanema Rivers, respectively aligned in the West-East and North-South directions, and the 800 m Araçoiaba Hills in the South-West of the CEA.

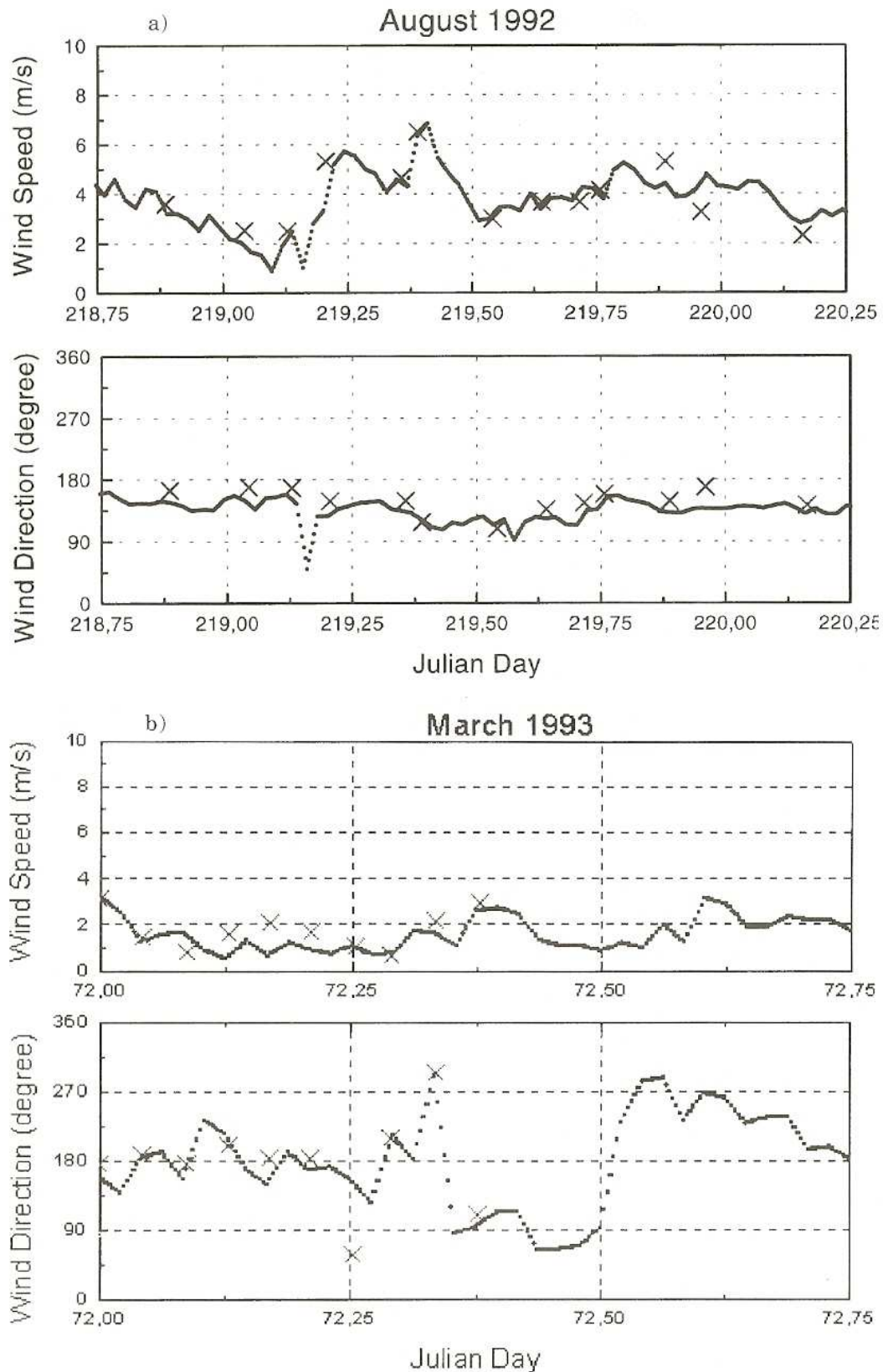


Fig. 2. – a) Time evolution of wind speed (above) and wind direction (below) measured at 11.5 m during the winter season at Iperó, SP, Brazil. The winter period corresponds to 36 hours from 18:00 LT on August 5 to 06:00 LT (Local Time) on August 7, 1992. The crosses correspond to tethered balloon sounding values interpolated at 10 m. b) Time evolution of wind speed (above) and wind direction (below) measured at 11.5 m during the winter season at Iperó. The summer period corresponds to 18 hours, from 00:00 to 18:00 LT on March 13, 1993. The crosses correspond to tethered balloon sounding values interpolated at 10 m.

moisture and horizontal wind speed and direction were obtained every two hours using a tethered balloon. Radiosonde soundings were also available.

The campaigns took place during the winter season, in August 1992, and in the summer, in March 1993, and each one lasted two weeks. The surface was covered by short grass 0.3 m high in August and by 0.5 m corn in March. The corresponding roughness length (z_0), evaluated from the vegetation cover type and height [15], is 0.05 m for the winter and 0.10 m for the summer period. The average surface albedo, estimated from solar radiation measurements, is 0.21 ± 0.03 in August and 0.16 ± 0.03 in March. The soil thermal conductivity, estimated from measured soil temperatures and heat flux profiles, is $0.79 \pm 0.05 \text{ W m}^2/\text{km}^{-1}$ in August and $0.56 \pm 0.09 \text{ W m}^2/\text{km}^{-1}$ in March. The average soil heat capacity for both seasons is $2.3 \times 10^6 \text{ J m}^3 \text{ K}^{-1}$.

Summer is the rainy season in this region, with the rain falling mainly towards the end of the day. Most of the rain is associated with convective activity induced by both the high content of air moisture and intense radiative heating at the surface. High precipitation values are also observed during the passage of synoptic-scale low-pressure systems. Winter is the dry season, with most of the weather determined by cold front passages, causing a significant drop in air temperature.

To characterize the seasonal variation of the PBL on the local dispersion conditions, the following 36-hour period was taken as being representative of the winter conditions: from 18:00 LT on August 5 to 06:00 LT on August 7 (respectively, from Julian day 218.75 to 220.25). The summer conditions were represented by a period of 18 hours, from 00:00 LT to 18:00 LT on March 13, 1993 (respectively, from Julian day 72 to 72.75). No rain was observed during these two periods and the local PBL time evolution was not affected by any significant synoptic disturbance or cloud effects.

In the winter period the wind velocity varied between 1 m s^{-1} and 7 m s^{-1} and wind direction was from SE for much of the time (fig. 2a), which is a typical situation after the passage of a cold front. In the summer period winds were weaker, varying between 0.5 m s^{-1} and 4.2 m s^{-1} . The wind direction varied from S, during the night and morning, to NE in the afternoon (fig. 2b). This diurnal pattern is observed during other periods and is associated with topographic effects [16-19].

3. – Surface energy-budget model

The model here used was proposed by Deardorff [10] and basically involves a numerical solution of an abbreviated surface energy-budget equation (forced-restored two-layer model for heat and humidity in the soil) to obtain the time evolution of the temperature and humidity representative of the surface covered by a vegetation layer.

TABLE I. – *Parameters used in the surface energy-budget model.*

Parameter	August 1992	March 1993
Mean soil temperature in the deeper layer (K)	291.2	301.6
Volumetric concentration of soil moisture in the deeper layer	0.10	0.30
Roughness length (m)	0.05	0.10
Albedo	0.21	0.16
Soil thermal diffusivity ($10^{-6} \text{ m}^2 \text{ s}^{-1}$)	0.33	0.24

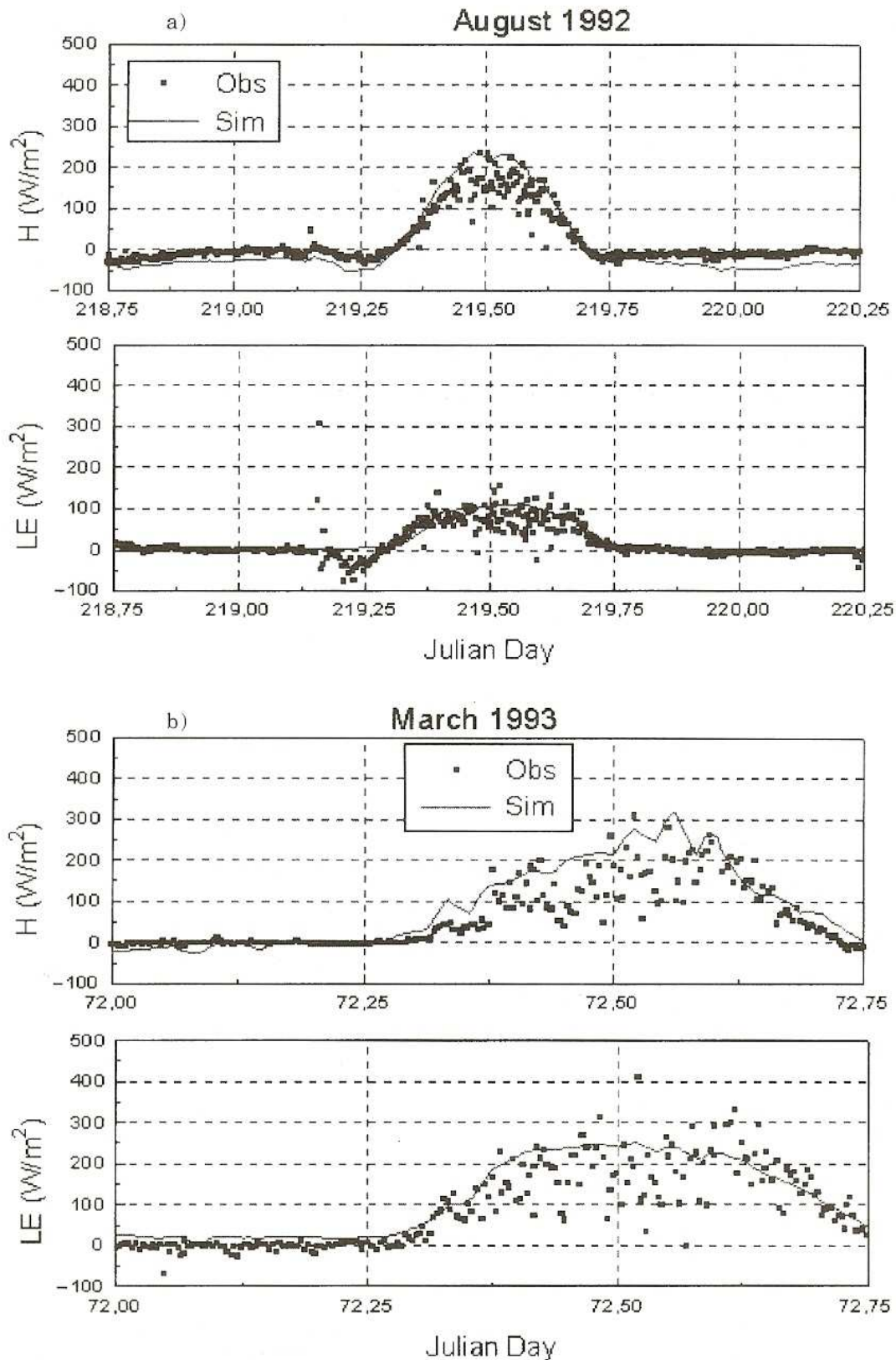


Fig. 3. – a) Time evolution of sensible heat flux (above) and latent heat flux (below), simulated (continuous) and measured (dotted), during the winter season at Iperó, SP, Brazil. The winter period corresponds to 36 hours from 18:00 LT on August 5 to 06:00 on August 7, 1992. b) Time evolution of sensible heat flux (above) and latent heat flux (below), simulated (continuous) and measured (dotted), during the summer season at Iperó. The summer period corresponds to 18 hours, from 00:00 to 18:00 LT on March 13, 1993.

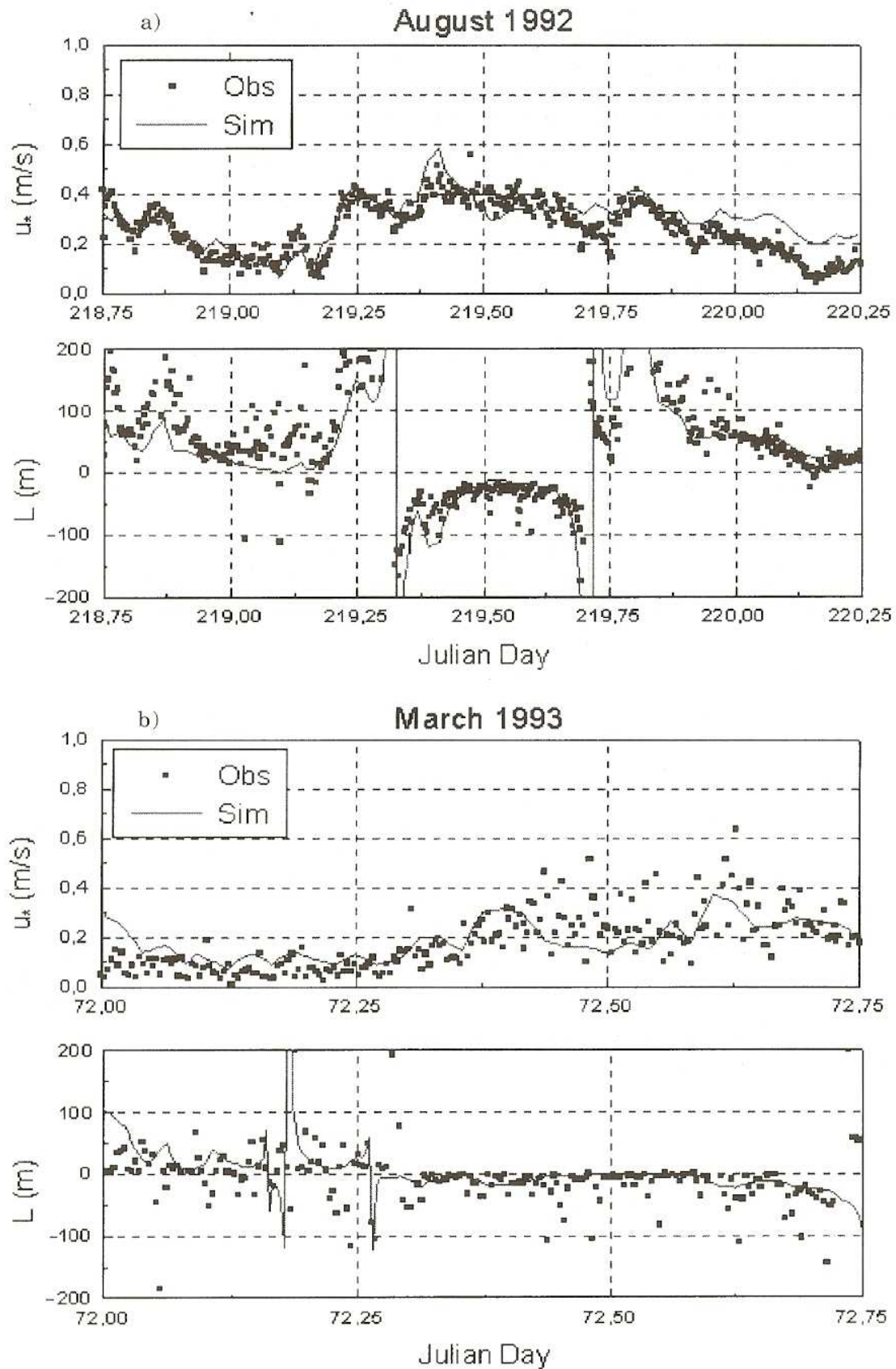


Fig. 4. – a) Time evolution of friction velocity (above) and the Monin-Obukhov length (below), simulated (continuous) and measured (dotted), during the winter season at Iperó. The winter period corresponds to 36 hours from 18:00 LT on August 5 to 06:00 LT on August 7, 1992. b) Time evolution of friction velocity (above) and the Monin-Obukhov length (below), simulated (continuous) and measured (dotted), during the summer season at Iperó. The summer period corresponds to 18 hours, from 00:00 LT to 18:00 LT on March 13, 1993.

The external parameters required to run this model are: air temperature, specific humidity and wind speed measured at one level above the surface (here assumed to be 10 m).

The internal parameters are estimated from observations, taking into account air turbulence measurements and the main characteristics of the heat and moisture transfer in the soil-vegetation interface. Table I shows the seasonal variation of the internal parameters estimated from the available observations at Iperó used in this study. The other internal parameters related to the vegetation were assumed to be similar to Deardorff [10], except for the foliage shielding factor, the surface emissivity and the depths of the soil affected by the diurnal and seasonal cycles of temperature, which were assumed to be constant and equal to 0.25, 0.95, 0.10 m and 0.5 m, respectively.

The time step used in the surface energy-budget model was equal to 5 minutes, corresponding to the frequency of the observed surface layer mean external parameters.

As can be seen in fig. 3, both sensible and latent fluxes match observations. The amplitude of the sensible and latent heat fluxes are greater in the summer, with maximum daytime values of 250 and 220 W/m², and lower in the winter with maximum daytime values of 220 W/m² and 100 W/m². During the night the sensible heat flux is negative and the latent flux slightly positive, with their magnitudes at least one order smaller than during the day.

During the chosen periods, friction velocity and Monin-Obukhov length have a time evolution typical of middle latitude continental areas. The low intensity of the wind is reflected in the low intensity of the friction velocity (below 0.10 m/s).

In qualitative terms, the results for both the winter and summer cases follow the observed time evolution of the surface layer turbulent fluxes, friction velocity and Monin-Obukhov length (figs. 3 and 4). To quantify this agreement between the model results and the observations the mean bias error, root mean standard error and t-statistic parameters, following Stone [20], are shown in table II. For a level of confidence of 99.9%, the critical t-statistic varies from 3.551 to 3.2991, for a degree of freedom of 40 and infinity, respectively. Thus, with the exception of the friction velocity on March 1993, the model results are comparable with observations. Despite the slight

TABLE II. - Mean Bias Error (MBE), Root Mean Standard Deviation (RMSE) and t-statistic [20] for a sample of size N . The parameter $d_i = (X_{\text{Sim}} - X_{\text{Obs}})$ is the difference between the simulated (X_{Sim}) and observed (X_{Obs}).

Parameter (X)	MBE $\left(\frac{1}{N} \sum_{i=1}^N d_i\right)$	RMSE $\left(\sqrt{\frac{1}{N} \sum_{i=1}^N (d_i)^2}\right)$	N	t-statistic $\left(\left[\frac{(N-1) \text{MBE}^2}{\text{RMSE}^2 - \text{MBE}^2}\right]^{1/3}\right)$
H_{August}	- 4.80	17.87	102	3.37
H_{March}	+ 7.69	38.39	48	1.40
LE_{August}	+ 6.20	19.48	102	2.80
LE_{March}	- 1.01	40.74	48	0.17
u^*_{August}	+ 0.0068	0.067	107	1.05
u^*_{March}	- 0.0850	0.120	56	7.34
L_{August}	26.40	461.5	107	0.58
L_{March}	58.36	385.6	56	1.14

overestimation (MBE positive), the performance of the model is better, reproducing the observed friction velocity and Monin-Obukhov length in the winter due to the higher intensity of the winds in this period.

4. – PBL height

During daytime, the height of the PBL (h) was estimated from a simplified version of the Mixed Layer model [12], as a function of the stability of the free atmosphere (γ_θ) and the surface heat flux $(\overline{\theta'w'})_0$:

$$(1) \quad h(t) = \left(\frac{14}{5} \frac{\int_{t_0}^t (\overline{\theta'w'})_0 dt}{\gamma_\theta} \right)^{1/2}.$$

The stability values of the free atmosphere, estimated from radiosonde soundings, were 0.004 K/m for both seasons (fig. 5a).

At night, the PBL height was estimated from equilibrium expressions proposed by Garratt [21] and Venkatram [11]:

$$(2) \quad h = \begin{cases} \gamma_c (u_* L / |f|)^{0.5}, & L < 100 \text{ m}, \\ cu_*^{1.5}, & L \geq 100 \text{ m}, \end{cases}$$

where $\gamma_c = 0.5$, $f = 0.000058 \text{ s}^{-1}$ for the latitude of Iperó ($\phi = 23.41^\circ\text{S}$) and $c = 2400 \text{ m}^{-1/2} \text{ s}^{3/2}$. The Venkatram expression was used during the transition period when the Monin-Obukhov length was greater than 100 m, while Garrat's expression was employed when the Monin-Obukhov length was less than 100 m.

The above expressions are coupled with the surface model to generate the PBL height as a function of the sensible heat flux, friction velocity and Monin-Obukhov length.

The diurnal variation of the PBL height was estimated using vertical soundings. During the daytime, the height of convective PBL was identified as the base of the elevated temperature inversion layer for the radiosonde soundings (fig. 5a). Unfortunately, the tethered balloon soundings were nearly always below the top of the convective PBL. In such cases, the values indicated as PBL height (identified by the symbol ">" in column z_i in tables III and IV and "x" in fig. 6a) should be interpreted as an indication that the convective PBL does exist and its top is above this height.

During the nighttime, the height of the stable PBL was identified as the height where the gradient Richardson Number (Ri) reaches a value equal to 1 by the first time (h_{Ri}). The Ri was evaluated for each sounding using interpolated wind speed (zonal and meridional components) and potential temperature. The interpolation [22] was carried out with a polynomial of degree 6 yielding smoother and more representative profiles of the atmosphere mean state than the tethered balloon soundings (fig. 5b).

Alternatively, following the criteria used by Marht *et al.* [23], the vertical extent of the PBL was also estimated as the height where the wind speed reaches the first maximum value (h_{Vel}). This was accomplished by identifying the height where the Ri reaches its first maximum (Ri_{max}), as indicated in fig. 5b. As can be seen in tables III

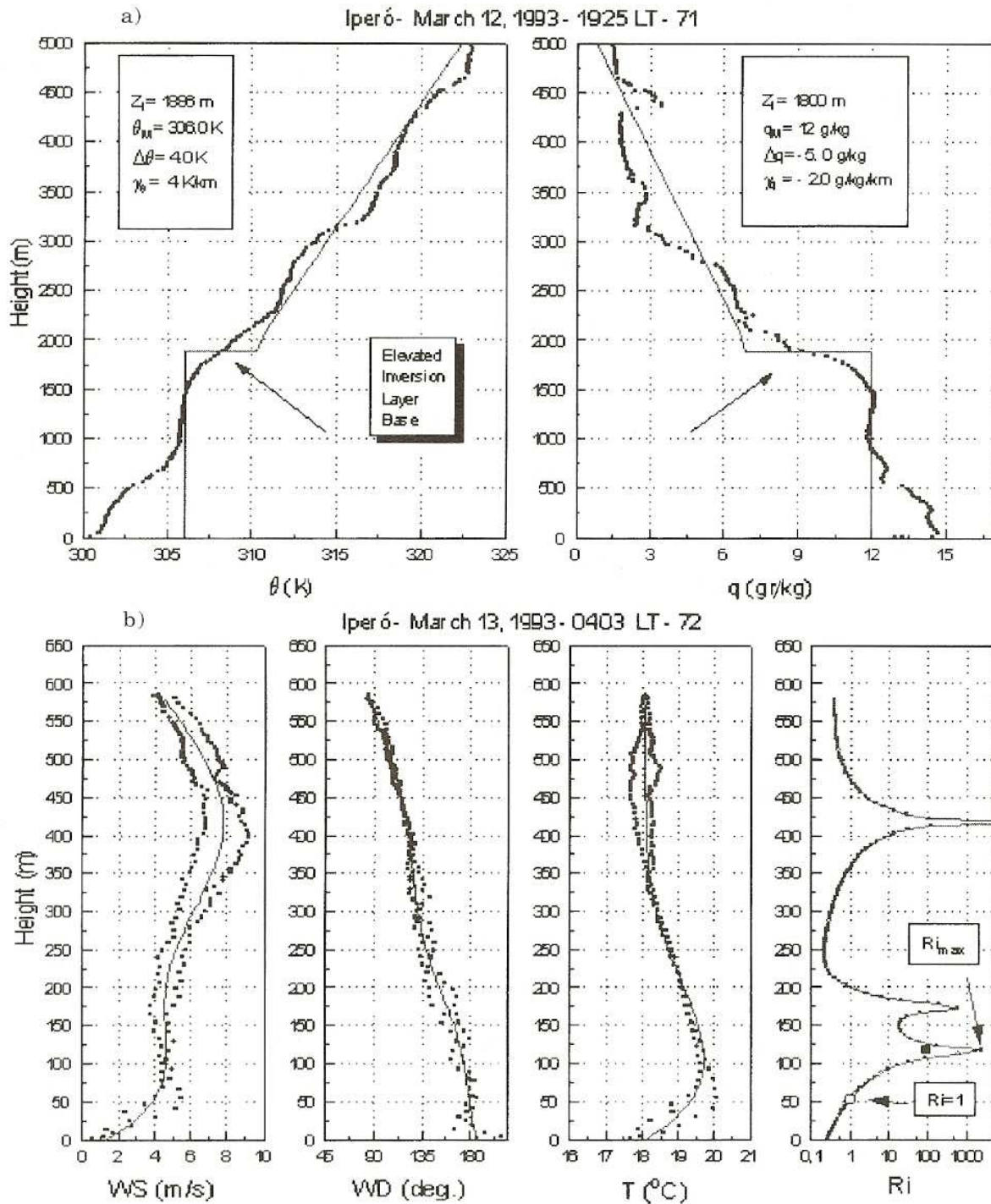


Fig. 5. – a) Vertical profile of potential temperature (left) and specific humidity of the air (right). Radiosonde sounding carried out on March 12, 1993, at 19:25 LT. The measured values are indicated by dots and the interpolated values are indicated by a continuous line. The symbols: Z_i , θ_M , $\Delta\theta$ and γ_θ are the PBL height, Mixed-Layer potential temperature, intensity of the inversion layer and the lapse rate, respectively. The symbols: q_M , Δq and γ_q are the Mixed-Layer value, intensity of the inversion layer and the lapse rate for the specific humidity. b) Vertical profile of wind speed (left), wind direction (left-center), air temperature (right-center) and Gradient Richardson Number (right). Tethered balloon sounding carried out on March 13, 1993, at 04:03 LT. The measured values are indicated by dots and the interpolated values are indicated by a continuous line.

TABLE III. – PBL height estimated from tethered balloon soundings for the winter period in Iperó.

Date	Julian Day	Local time	h_{Ri} (m)	h_{Vel} (m)	z_i (m)
08.05.1992	218.90	21:15	69.9	90.	—
08.06.1992	219.04	01:00	53.1	120.	—
08.06.1992	219.13	03:05	81.1	170.	—
08.06.1992	219.19	04:55	42.8	85.	—
08.06.1992	219.35	08:30	—	—	> 235
08.06.1992	219.39	09:15	—	—	> 165
08.06.1992	219.54	12:52	—	—	> 515
08.06.1992	219.64	15:15	—	—	> 515
08.06.1992	219.75	18:03	97.5	140.	—
08.06.1992	219.88	21:15	164.5	180.	—
08.06.1992	219.96	23:00	> 125.	> 125.	—
08.07.1992	220.15	03:55	148.7	172.5	—
08.07.1992	220.25	06:05	134.8	167.5	—

TABLE IV. – PBL height estimated from tethered balloon and radiosonde soundings for the summer period in Iperó.

Date	Julian Day	Local time	h_{Ri} (m)	h_{Vel} (m)	z_i (m)
03.12.1993	71.75	18:00	97.91	112.5	—
03.12.1993	71.81	19:25	—	—	1886
03.12.1993	71.91	21:54	68.73	82.73	—
03.12.1993	71.96	23:04	55.32	102.50	—
03.13.1993	72.00	00:00	13.5	32.5	—
03.13.1993	72.04	01:00	51	117.5	—
03.13.1993	72.09	02:04	0	0.	—
03.13.1993	72.13	03:03	0	0.	—
03.13.1993	72.17	04:03	52.0	117.5	—
03.13.1993	72.21	05:02	49.1	127.5	—
03.13.1993	72.25	06:04	74.4	107.5	—
03.13.1993	72.29	06:56	73.7	107.5	—
03.13.1993	72.33	08:00	—	—	300

and IV, the two methods are equivalent for summer and winter periods. It was also found, in agreement with Marht *et al.* [23], that $h_{\text{Vel}} > h_{\text{Ri}}$.

The time evolutions of the observed PBL height are shown in figs. 6a and b, respectively, for winter and summer periods. The PBL height during nighttime is closely related to the wind speed and, in spite of the more intense nighttime cooling, the PBL height is higher in the winter when the wind speed is greater. It is important to emphasize that the wind speed measured by a Gill anemometer on the tower at 11.5 m (dotted line in fig. 2), used as an external parameter in surface-budget model, compares well with the wind measured by tethered balloon at 10 m (crosses in fig. 2), used to estimate the Richardson Number profiles and the height of the stable PBL.

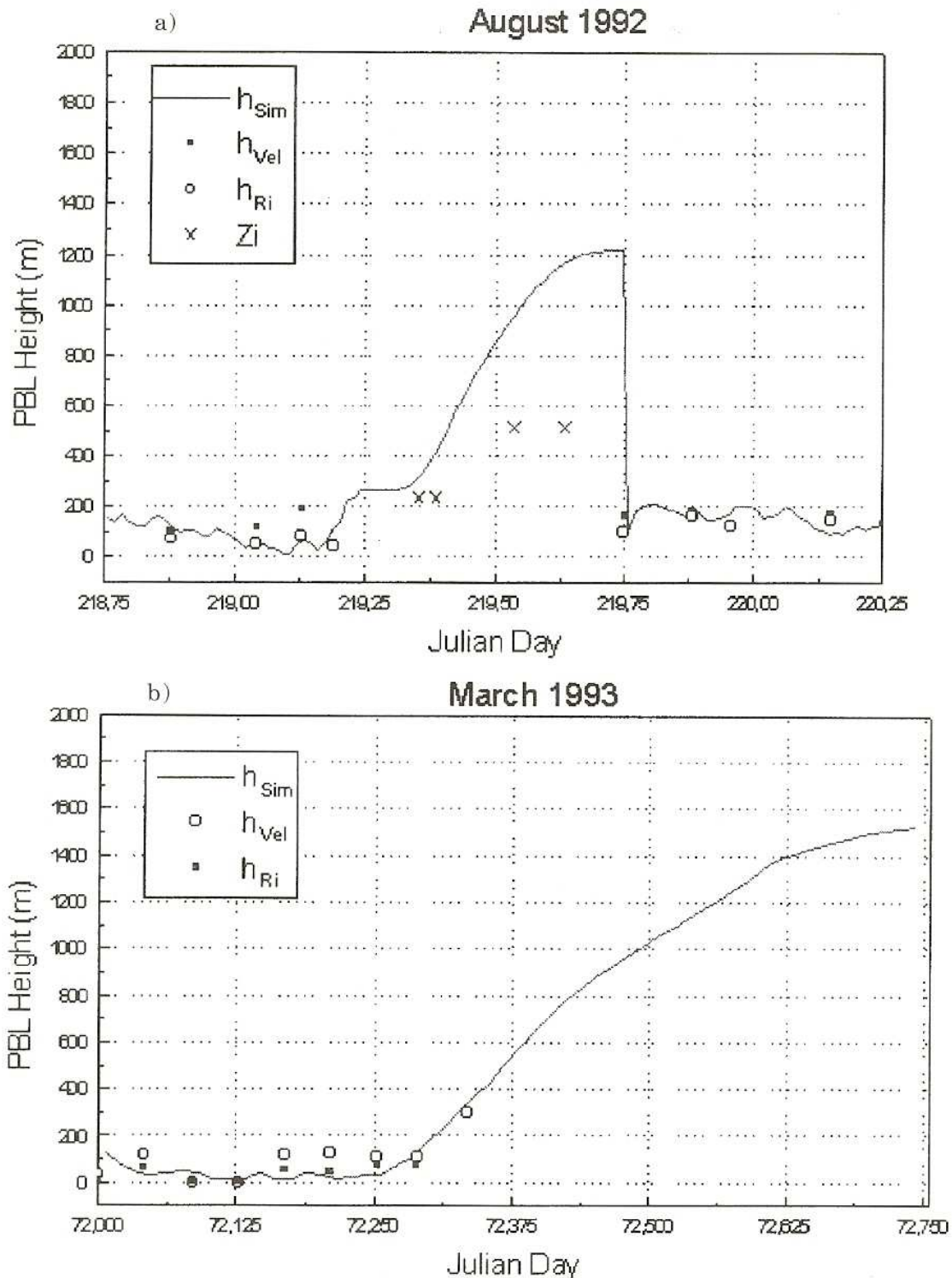


Fig. - 6. a) Time evolution of the PBL height for the winter season at Iperó. The winter period corresponds to 36 hours from 18:00 LT on August 5 to 06:00 LT on August 7, 1992. b) Time evolution of the PBL height for the summer season at Iperó. The summer period corresponds to 18 hours, from 00:00 LT to 18:00 LT on March 13, 1993.

5. - Diffusion model

The SPM is a time-dependent puff model based on the Monin-Obukhov similarity theory and approximated solutions proposed by van Ulden [24,25] for the diffusion

equation. In this model, the interaction between vertical wind shear and diffusion is treated explicitly to take into consideration that the dispersion of a cloud of passive contaminant released from a source near the ground is strongly determined by skewness effects induced by the wind shear near the surface.

The model performance was evaluated against tracer data of two different experimental data sets [24]: the Prairie Grass data set [26], for an emission source near the ground (as in the case of the present paper), and the Copenhagen data set [27], for a relatively high source.

The SPM simulations were carried out using as input 5 minute-averaged wind speed and direction observed at 11.5 m, friction velocity and Monin-Obukhov length supplied by the surface energy-budget model, and the PBL height estimated from empirical equilibrium expressions for the nighttime and the Mixed Layer model for the daytime.

The time-integrated radionuclide concentration field at the surface was estimated for both summer and winter conditions, considering a hypothetical accident at Iperó,

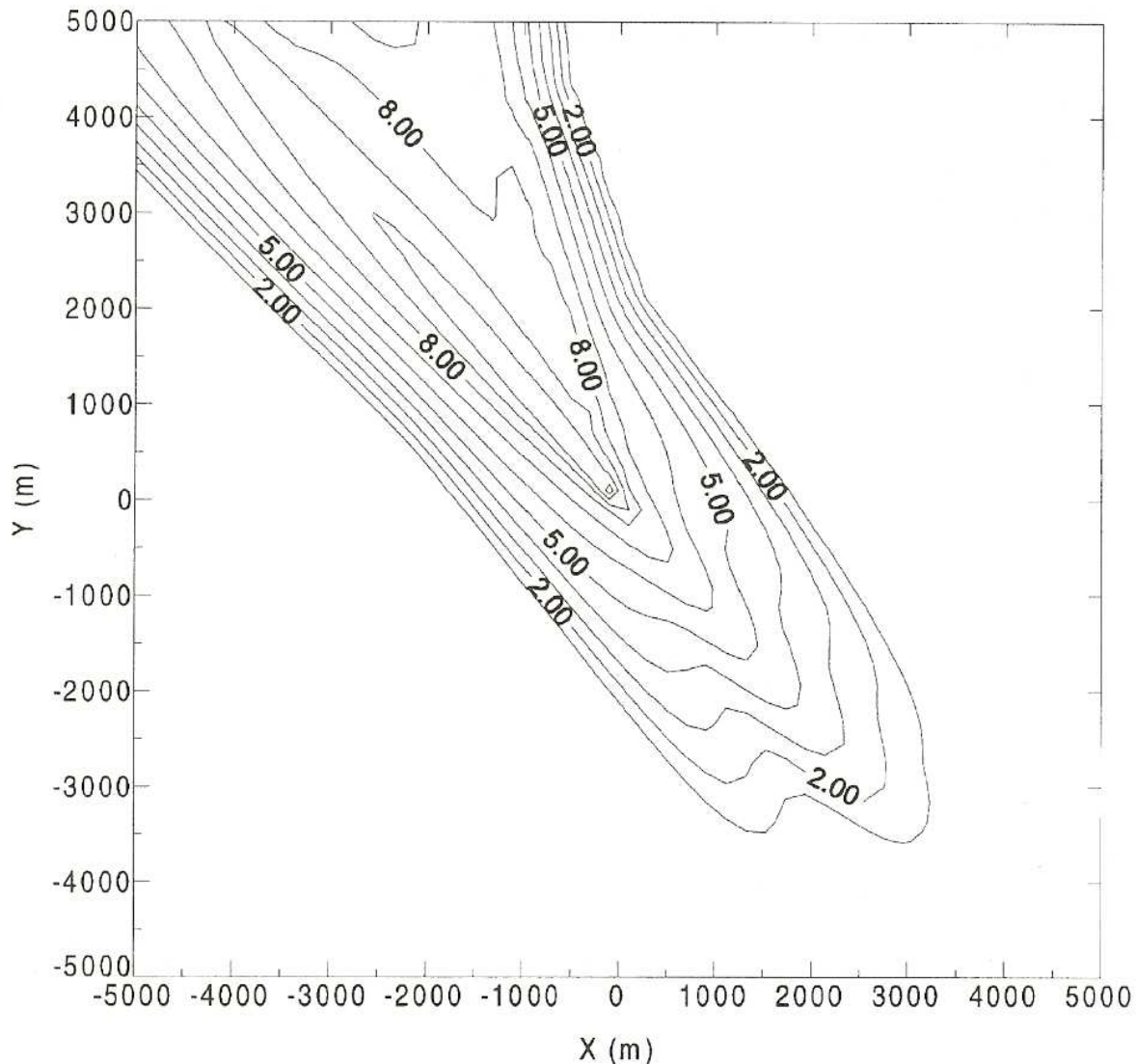


Fig. 7. – Isolines of the logarithm of hour average ground-level concentration normalized by the emission flux (10^{-15} s/m^3) over the complete period of 36 hours for the winter season at Iperó. The source is located at the coordinate point (0,0), 10 m above the surface and the emission is continuous and constant in time.

producing a continuous emission from a 10 m height point source for 18 hours during the summer and 36 hours during the winter.

6. – Results and conclusion

The atmospheric diffusion from a hypothetical release of radionuclides in the region of Iperó, Brazil, was simulated with the SPM. It considered a point source located near the surface (10 m), emitting continuously, and a PBL horizontally homogeneous within the domain of 10 by 10 km.

The required parameters to run the SPM are: wind speed and direction at one level, roughness length, friction velocity, Monin-Obukhov length and the PBL height.

The wind speed and direction are provided by observations (5 min average) carried out during the turbulence field campaigns at Iperó. PBL height, friction velocity and Monin-Obukhov length were estimated using a surface energy-budget model coupled with a semi-empirical formula.

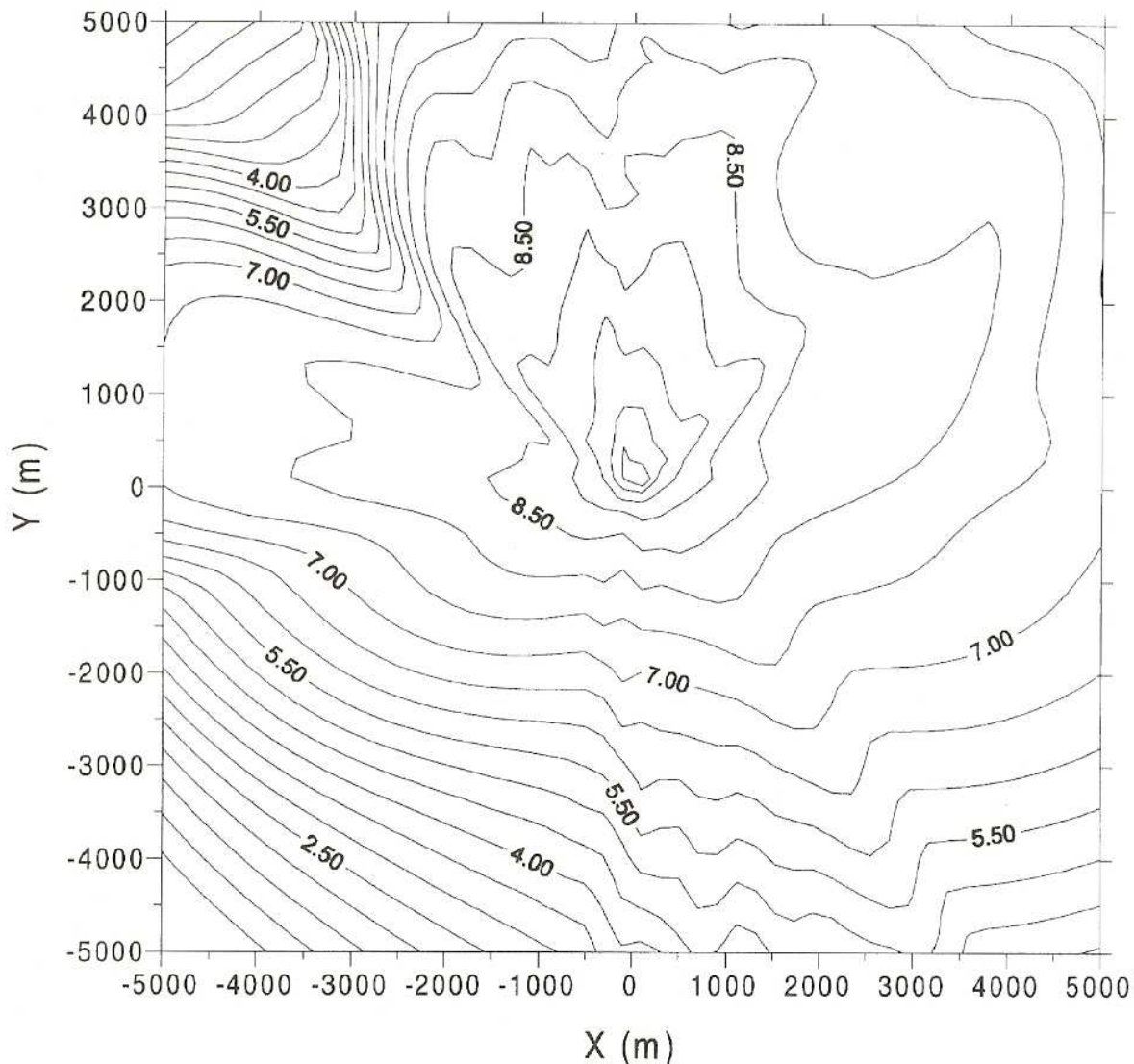


Fig. 8. – Isolines of the logarithm of mean ground-level concentration normalized by the emission flux (10^{-15} s/m³) over the complete period of 48 hours for the summer season. The source is located at the co-ordinate point (0,0), 10 m above the surface and the emission is continuous and constant in time.

The surface layer turbulence data and vertical profiles in the PBL provided the information required to calibrate the surface energy-budget model and the empirical expressions used to estimate the PBL height.

The agreement between the observed and simulated sensible and latent heat fluxes, friction velocity and Monin-Obukhov length, within a level of confidence of 99.9%, indicates that the internal parameters chosen for the surface energy-budget model are representative of the interface soil-vegetation conditions at Iperó for both summer and winter seasons.

The mean ground level concentration isolines shown in figs. 7 and 8 were normalized by the source emission (in units of 10^{-5} s/m³) and correspond to the situation after a continuous emission of 36 hours during the winter (from 18:00 LT on August 5 to 06:00 LT on 7 of August, 1992) and 18 hours (from 00:00 LT to 18:00 LT on March 13 of 1993) during summer period.

These results show that, in both seasons, the highest concentration values are located near to the source and that most of the contaminated area is within a 5 kilometers range. In winter, the contaminated area is elongated in the NW-SE direction, NW of the source, with a cone-shaped appearance. In the summer period, the shape of the plume is more symmetrical with respect to the source position. These results indicate that the concentration field is strongly affected by the seasonal variation of wind. In the winter period the wind speed is comparatively higher and the wind direction more constant (145 degrees). The highly variable wind direction and smaller wind speed are an indication that the dispersion in the summer case is ruled by the daytime convective PBL vertical evolution (fig. 6b).

* * *

The authors acknowledge the financial support provided by the Brazilian "Conselho Nacional de Desenvolvimento Científico e Tecnológico - CNPq" and the Italian "Consiglio Nazionale delle Ricerche - CNR" for the international collaboration program during 1994-97.

REFERENCES

- [1] WEIL J. C., *J. Clim. Appl. Meteor.*, **24** (1985) 1111-1130.
- [2] BERKOWICZ R. R., OLESEN H. R. and TORP U., *Proceedings of the NATO-CCMS 16th International Meeting on Air Pollution Modelling and Its Applications*, edited by C. DE WISPELAERE, F. A. SCHIERMEIER and N. V. GILLANI (Plenum Press, New York) 1986, pp. 453-481.
- [3] TIRABASSI T., *Water, Air Soil Poll.*, **47** (1989) 19-24.
- [4] HANNA S. R. and PAINE R. J., *J. Appl. Meteor.*, **28** (1989) 206-224.
- [5] HOLTSLAG A. A. M. and VAN ULDEN A. P., *J. Clim. Appl. Meteor.*, **22** (1983) 517-529.
- [6] VAN ULDEN A. P. and HOLTSLAG A. A. M., *J. Clim. Appl. Meteor.*, **24** (1985) 1196-1207.
- [7] TROMBETTI F., TAGLIAZUCCA M., TAMPIERI F. and TIRABASSI T., *Atmos. Environ.*, **20** (1986) 2465-2471.
- [8] HOLTSLAG A. A. M. and DE BRUIN H. A. R., *J. Appl. Meteor.*, **27** (1988) 689-704.
- [9] BELJAARS A. C. M. and HOLTSLAG A. A. M., *Environ. Soft.*, **5** (1990) 60-68.
- [10] DEARDORFF J. W., *J. Geophys. Res.*, **83** (1978) 1889-1903.
- [11] VENKATRAM A., *Boundary Layer Meteorology*, **19** (1980) 481-485.
- [12] TENNEKES H., *J. Atmos. Sci.*, **30** (1973) 558-581.

- [13] OLIVEIRA A. P., DEGRAZIA G. A., MORAES O. L. L. and GOEDERT J., *Proceedings of the Symposium Nuclear Energy and Environment, Rio de Janeiro, 28 June-1 July 1993* (Latin American Section/American Nuclear Society) 1993, p. III.11-19.
- [14] OLIVEIRA A. P., MORAES O. L. L., DEGRAZIA G. A. and DE MOLNARY L., *Rev. Brasil. Geofis.*, **12** (1994) 55-58.
- [15] PANOFKY H. A. and DUTTON J. A., *Variances of Turbulence Characteristics in: Atmospheric Turbulence Models and Methods for Engineering Applications* (J. Willey) 1984, Chapt. 7, pp. 160-162.
- [16] TIRABASSI T., DE OLIVEIRA A. P., ANDRADE M. F., MORAES O. L. L., DEGRAZIA G. A., *AER*, **1** (1996) 4-6.
- [17] KARAM H. A., *Simulação Numérica Tridimensional da Camada Limite Planetária em Iperó*, São Paulo, Dissertação de Mestrado, Departamento de Ciências Atmosféricas - IAG/USP, 1995, pp. 112 (in Portuguese).
- [18] OLIVEIRA A. P., DEGRAZIA G. A., MORAES O. L. L. and TIRABASSI, *Third International Conference on Air Pollution 95, September 26-29, 1995, Porto Carras, Greece*, Vol. 1, edited by H. POWER, N. MOUSSIOPOULOS and C. A. BREBBIA (Computational Mechanics Publications, Southampton) 1995, pp. 167-174.
- [19] MOLNARY L., *Caracterização de um modelo de camada limite planetária para avaliar liberações de radionuclédeos em instalações nucleares*. Dissertação de Mestrado, Departamento de Ciências Atmosféricas - IAG/USP, 1994, pp. 122 (in Portuguese).
- [20] STONE R. J., *Solar Energy*, **51** (1993) 289-291.
- [21] GARRAT J. R., *Bound.-Layer Meteor.*, **22** (1981) 21-48.
- [22] PRESS W. H., FLANNERY B. P., TAUKOLSKY S. A. and VETTERLING W. T., *Numerical Recipes, The Art of Scientific Computing* (Cambridge University Press) 1986.
- [23] MARHT L., HEALD R. C., LENSCHOW D. H., STANKOV B. B. and TROEN I. B., *Bound.-Layer Meteor.*, **17** (1979) 247-264.
- [24] TIRABASSI T. and RIZZA U., *J. Appl. Meteor.*, **34** (1995) 989-993.
- [25] VAN ULDEN A. P., *Atmos. Environ.*, **26 A** (1992) 681-692.
- [26] BARAD M. L., Report AFCRL-TR-235, 1985.
- [27] GRYNING S. E. and LYCK E., *J. Clim. Appl. Meteor.*, **23** (1984) 651-660.